Acknowledgments

We thank Michael Hann (Florida International University) for critical comments and language editing, Rie Tanaka, Hisae Nakagawa, Tomoko Sasaki, Sanae Hayashi (The University of Tokushima) for excellent technical assistance and Yoko Okazawa, Akiyo Muramoto (The University of Tokushima) for clinical assistance.

Author Contributions

Conceived and designed the experiments: KN HA TD. Performed the experiments: KN M. Miyoshi TT. Analyzed the data: KN. Contributed reagents/materials/analysis tools: KN TK NF M. Matsuura ES SY KY HK TF KY HI AM NA TA TM FK SK TM HA. Wrote the paper: KN.

References

1. Yanagita M, Arai H, Ishii K, Nakano T, Ohashi K, et al. (2001) Gas6 regulates mesangial cell proliferation through Axl in experimental glomerulonephritis. Am J Pathol 158: 1423–1432.
2. Yanagita M, Ishimoto Y, Arai H, Nagai K, Ito T, et al. (2002) Essential role of Gas6 for glomerular injury in nephrotoxic nephritis. J Clin Invest 110: 239–246.
3. Nagai K, Arai H, Yanagita M, Matsubara T, Kanamori H, et al. (2003) Growth arrest-specific gene 6 is involved in glomerular hypertrophy in the early stage of diabetic nephropathy. J Biol Chem 278: 18229–18234.
4. Nagata K, Ohashi K, Nakano T, Arita H, Zong C, et al. (1996) Identification of the product of growth arrest-specific gene 6 as a common ligand for Axl, Sky, and Mer receptor tyrosine kinases. J Biol Chem 271: 30022–30027.
5. Yanagita M, Ishii K, Ozaki H, Arai H, Nakano T, et al. (1999) Mechanism of inhibitory effect of warfarin in mesangial cell proliferation. J Am Soc Nephrol 10: 2503–2509.
6. Funakoshi H, Yonemasu T, Nakano T, Matumoto K, Nakamura T (2002) Identification of Gas6, a putative ligand for Sky and Axl receptor tyrosine kinases, as a novel neurotrophic factor for hippocampal neurons. J Neurosci Res 68: 150–160.
7. Crosier KE, Hall LR, Lewis PM, Morris CM, Wood CR, et al. (1994) Isolation and characterization of the human Dtk receptor kinase. Growth Factors 11: 137–144.
8. Nystrom J, Fierlbeck W, Granqvist A, Kulak SC, Ballermann BJ (2009) A human glomerular SAGE transcriptome database. BMC Nephropathy 10: 13.
9. Tumlin JA, Madaio MP, Hennigar R (2007) Idiopathic IgA nephropathy: Pathogennesis, histopathology, and therapeutic options. Clin J Am Soc Nephrol 2: 1054–1061.
10. D'Amico G (2004) Natural history of idiopathic IgA nephropathy and factors predictive of disease outcome. Semin Nephrol 24: 179–196.
11. A Working Group of the International IgA Nephropathy Network and the Renal Pathology Society (2009) The Oxford classification of IgA Nephropathy: pathology definitions, correlations, and reproducibility. Kidney Int 76: 546–556.
12. A Working Group of the International IgA Nephropathy Network and the Renal Pathology Society (2009) The Oxford classification of IgA Nephropathy: rationale, clinicopathoogical correlations, and classification. Kidney Int 76: 534–545.
13. Shankland SJ, Hugo C, Coats SR, Nangaku M, Pichler RH, et al. (1996) Changes in cell-cycle protein expression during experimental mesangial proliferative glomerulonephritis. Kidney Int 50: 1230–1239.
14. Qju LQ, Sinniah R, Hsu SI (2004) Role of differential and cell type-specific expression of cell cycle regulatory proteins in mediating progressive glomerular injury in human IgA nephropathy. Lab Invest 84: 1112–1125.
15. Matsuo S, Imai E, Horio M, Yasuda Y, Tomita K, et al. (2009) Revised equations for estimated GFR from serum creatinine in Japan. Am J Kid Dis 53: 982–992.
16. Tominaga T, Abe H, Ueda O, Goto C, Nakahara K, et al. (2011) Activation of BMP4 signaling leads to glomerulosclerosis that mimics diabetic nephropathy. J Biol Chem 286: 20109–20116.
17. Mundel P, Reiser J, Zúñiga Mejía Borja A, Pavenstädt H, Davidson GR, et al. (1997) Rearrangements of the cytoskeleton and cell contacts induce process formation during differentiation of conditionally immortalized mouse podocyte cell lines. Exp Cell Res 236: 248–258.
18. Murakami T, Abe H, Nagai K, Tominaga T, Takamatsu N, et al. (2010) Trophoblast glycoprotein: possible candidate mediating podocyte injuries in glomerulonephritis. Am J Nephrol 32: 505–521.
19. Demarchi F, Verardo R, Varnum B, Brancolini C, Schneider C (2001) Gas6 anti-apoptotic signaling requires NF-kappa B activation. J Biol Chem 276: 31738–31744.
20. O'Donnell K, Harkes IC, Dougherty L, Wicks IP (1999) Expression of receptor tyrosine kinase Axl and its ligand Gas6 in rheumatoid arthritis: evidence for a novel endothelial cell survival pathway. Am J Pathol 154: 1171–1180.
21. Graham DK, Dawson TL, Mullaney DL, Snodgrass HR, Earp HS (1994) Cloning and mRNA expression analysis of a novel human protooncogene, c-mer. Cell Growth Differ 5: 647–657.
22. Chen J, Carey K, Godowski PJ (1997) Identification of Gas6 as a ligand for Mer, a neural cell adhesion molecule related receptor tyrosine kinase implicated in cellular transformation. Oncogene 14: 2033–2039.
23. Asao R, Asanuma K, Kodama F, Akiba-Takagi M, Nagai-Hosoe Y, et al. (2012) Relationships between levels of urinary podocalyxin, number of urinary podocytes, and histologic injury in adult patients with IgA nephropathy. Clin J Am Soc Nephrol 7: 1385–1393.
24. Peters HP, Waanders F, Meijer E, van den Brand J, Steenbergen EJ, et al. (2011) High urinary excretion of kidney injury molecule-1 is an independent predictor of end-stage renal disease in patients with IgA nephropathy. Nephrol Dial Transplant 26: 3581–3588.
25. Xu PC, Zhang JJ, Chen M, Lv JC, Liu G, et al. (2011) Urinary kidney injury molecule-1 in patients with IgA nephropathy is closely associated with disease severity.Nephrol Dial Transplant 26: 3229–3236.
26. Ding H, He Y, Li K, Yang J, Li X, et al. (2007) Urinary neutrophil gelatinase-associated lipocalin (NGAL) is an early biomarker for renal tubulointerstitial injury in IgA nephropathy. Clin Immunol 123: 227–234.
27. Zhao N, Hou P, Lv J, Moldoveanu Z, Li Y, et al. (2012) The level of galactose-deficient IgA1 in the sera of patients with IgA nephropathy is associated with disease progression. Kidney Int 82: 790–796.
28. Onda K, Ohsawa I, Ohi H, Tamano M, Mano S, et al. (2011) Excretion of complement proteins and its activation marker C5b-9 in IgA nephropathy in relation to renal function. BMC Nephrol 12: 64.
29. Liu LL, Jiang Y, Wang LN, Liu N (2012) Urinary mannose-binding lectin is a biomarker for predicting the progression of immunoglobulin (Ig)A nephropathy. Clin Exp Immunol 169: 148–155.
30. Ebefors K, Granqvist A, Ingelsten M, Mölne J, Haraldsson B, et al. (2011) Role of glomerular proteoglycans in IgA nephropathy. PLoS One 6: e18575.

Clin Exp Nephrol (2013) 17:882–889
DOI 10.1007/s10157-013-0785-9

ORIGINAL ARTICLE

Polymorphism in the human matrix Gla protein gene is associated with the progression of vascular calcification in maintenance hemodialysis patients

Kazuhiro Yoshikawa · Hideharu Abe · Tatsuya Tominaga · Masayuki Nakamura · Seiji Kishi · Motokazu Matsuura · Kojiro Nagai · Kenji Tsuchida · Jun Minakuchi · Toshio Doi

Received: 6 September 2012 / Accepted: 13 February 2013 / Published online: 16 March 2013

Abstract
Background Matrix Gla protein (MGP) is one of the important proteins inhibiting vascular calcification (VC). Single nucleotide polymorphisms (SNPs) located in the promoter and coding regions of the *MGP* gene affect the transcriptional activity. In this study, we investigated the relationship between the SNPs and progression of VC in patients undergoing maintenance hemodialysis (MHD).
Methods This was a retrospective, longitudinal cohort study of 134 MHD patients whose VC could be followed by multi-detector computed tomography (MDCT) examinations. MGP-SNPs (T-138C, rs1800802 and G-7A, rs1800801) were determined. The progression speed of VC was examined by plotting the abdominal aortic calcium volume scores.
Results The progression speed of VC of patients with the CC genotype of T-138C was significantly slower than that of patients with the CT or TT genotype. Multiple regression analysis showed that CT/TT genotype, greater age at the beginning of MHD, male sex, high levels of calcium × phosphate, low levels of high-density lipoprotein cholesterol, high levels of low-density lipoprotein cholesterol, low levels of ferritin and non-use of angiotensin II receptor blockers were significantly associated with progression of VC.
Conclusions The MGP-138CC genotype may be associated with slower progression of VC in MHD patients. The genotype of the *MGP* gene will be a genomic biomarker that is predictive of VC progression.

Keywords Matrix Gla protein (MGP) · Abdominal aortic calcium volume score (AACVS) · Single nucleotide polymorphisms (SNPs)

K. Yoshikawa · H. Abe (✉) · T. Tominaga · S. Kishi · M. Matsuura · K. Nagai · T. Doi
The Department of Nephrology, Institute of Health Biosciences, University of Tokushima Graduate School, Tokushima 770-8503, Japan
e-mail: abeabe@clin.med.tokushima-u.ac.jp

M. Nakamura · K. Tsuchida · J. Minakuchi
The Department of Kidney Disease, Dialysis and Kidney Transplantation, Kawashima Hospital, Tokushima, Japan

Introduction

Vascular calcification (VC) is a common finding in patients undergoing maintenance hemodialysis (MHD). MHD patients have a 60–80 % prevalence of moderate to severe VC [1–3]. The VC often progresses over a relatively short period of time and is a strong predictor of cardiovascular disease and all-cause mortality in MHD patients [4–6]. Abdominal aortic calcification (AAC) is reported to be a predictor for cardiovascular mortality in the general population, and was also associated with increased risk of congestive heart failure in the Framingham Study. The association between AAC and all-cause and cardiovascular mortality in MHD patients has been shown in several reports. However, the factors contributing to AAC in MHD patients are still not fully understood.

Genetic and biochemical studies have established matrix Gla protein (MGP) as the first protein known to act as a calcification inhibitor in vivo. MGP is a vitamin K-dependent protein of 84 amino acids with a molecular weight of 12 kDa [7, 8]. Although MGP knockout mice are normal at birth, they rapidly develop severe arterial calcifications and subsequent vascular ruptures leading to death within 6–8 weeks [9]. Among three types of arteriosclerosis (i.e., atherosclerosis, Mönkeberg medial calcific

sclerosis, and arteriolosclerosis), arterial medial calcification is the major cause of vascular disease and is rapidly progressive in dialysis patients [2]. Therefore, MGP would be a critical factor in the development of arteriosclerosis in patients with MHD. A few previous reports have investigated serum MGP levels in hemodialysis patients, but the relationship between the serum MGP concentration and VC is controversial [10, 11].

It has been reported that the gene encoding MGP has several single nucleotide polymorphisms (SNPs) in its promoter and coding regions. Many studies have revealed the significance of *MGP* gene polymorphisms at T-138C and G-7A [12–14]. A previous study showed that MHD patients have a different distribution of *MGP* gene polymorphisms as compared with the normal population [14]. However, the influence of MGP polymorphism with respect to the development of AAC in MHD patients is not fully understood [12, 15]. It is a fact that there are no reports which examine the association between MGP polymorphism and AAC. With regard to 'femoral artery' calcification, Herrman et al. [12] reported that it was more prevalent in carriers of the MGP A-7 allele than in MGP GG-7 homozygotes and that T-138C were unrelated to femoral artery calcification in healthy volunteers. In addition, Crosier et al. [15] reported that in males, homozygous carriers of the minor allele of T-138C, G-7A and Ala102Thr were associated with a decreased quantity of 'coronary artery calcification (CAC)', relative to major allele carriers.

To date, the exact mechanisms for accelerated VC have yet to be fully determined. In particular, it is conceivable that the speed of progression of AAC in hemodialysis patients varies widely from patient to patient. Therefore, we examined whether MGP-SNPs affect the progression speed of AAC in MHD patients.

Materials and methods

Study design, setting and participants

This is a retrospective, longitudinal cohort study of MHD patients. As a setting, patients with end-stage kidney disease (ESKD) who started hemodialysis therapy after 2001 at Kawashima Hospital were recruited between August 2009 and November 2010. All of the procedures were performed in accordance with the guidelines of the Helsinki Declaration on Human Experimentation and the Ethical Guidelines on Clinical Research published by the Japanese Health, Labour and Welfare Ministry. This study was approved by the Ethics Committee of Tokushima University and Kawashima Hospital, and written informed consent was obtained from all patients.

The exclusion criteria were (1) past operation for abdominal aortic aneurysms and (2) renal transplantation.

Finally 145 participants were recruited and provided samples which we assayed for two SNPs in the *MGP* gene promoter region—T-138C (rs1800802) and G-7A (rs1800801). Routine abdominal computed tomography (CT) examination is performed once a year in each patient, and we used these data. We enrolled 134 of the 145 patients whose VC could be followed in consecutive multidetector CT (MDCT) examinations; 11 patients were excluded from additional analysis because they underwent MDCT examination once or not at all.

Identification of *MGP* gene genotypes

We selected two common SNPs on the *MGP* gene promoter—T-138C (rs1800802) and G-7A (rs1800801). Whole blood samples were obtained via vascular access at the start of routine hemodialysis treatment, and were used for the extraction of genomic DNA with a Wizard Genomic DNA Purification Kit (Promega, Madison, WI, USA). First, T-138C (rs1800802) polymorphism was genotyped using a mismatch polymerase chain reaction (PCR) fragment amplified with the primers for 142 bp region as a pilot study—5′-AAGCATACGATGGCCAAAACTTCTGCA-3′ and 5′-GAACTAGCATTGGAACTTTTCCCAACC-3′ [13]. These PCR products were purified with DNA Clean & Concentrator-5 kit (Zymo Research, Orange, CA, USA) and were digested with the restriction enzyme *Bsr*I, and analyzed in polyacrylamide gel (Fig. 1).

The following primers were designed for a 408 bp region that included T-138C (rs1800802) and G-7A (rs1800801)—5′-TCTGTCCCCAAGCATACGAT-3′ and 5′-ACACAGAGAAATGGGAGAAAAG-3′. These primers were verified by sequencing and PCR was carried out. Purified PCR products were subjected to direct sequencing by using 3730xl DNA Analyzer (Applied Biosystems).

Serum MGP assay

Serum MGP concentrations were quantified with a kit from Biomedica (Vienna, Austria) as described previously [16].

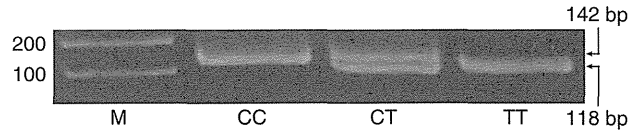

Fig. 1 Genotyping of the T-138C polymorphism using mismatch PCR followed by digestion with the restriction enzyme *Bsr*I. The presence of a T nucleotide at position −138 produced a *Bsr*I restriction endonuclease site giving fragments of 118 and 24 bp. The presence of a C nucleotide at position −138 did not produce a restriction endonuclease site for *Bsr*I. M: 100 bp DNA Ladder

Detection and measurement of VC

In order to evaluate the VC of each patient, we gathered data from the past abdominal CT examinations of each patient and calculated the abdominal aortic calcium volume score (AACVS). The plain abdominal MDCT imaging was performed using an 8-slice Aquarion scanner (Toshiba, Japan). The images from the bifurcation at the beginning of the common iliac artery to the 70-mm cranial interval were transferred to a workstation. Quantification of aortic calcification was carried out with ZIO Workstation software (ZIO, Japan). VC was defined as >130 Hounsfield units of CT value on this workstation, and counted as pixel data. The AACVS was defined according to the following formula—(pixel) × (pixel) × (slice thickness) × (quantity of voxel) [mm^3]. In this formula, (1 pixel) × (1 pixel) × (slice thickness) expresses (1 voxel). The volumetric scoring method named the calcium volume score was referred to in previous articles [17–19].

Statistical methods

We considered two-tailed p values <0.05 as statistically significant. All of the statistical analyses were performed using JMP 9.02 (SAS Institute, Cary, NC, USA). Statistical analysis of continuous variables was performed with Kruskal–Wallis analysis because assumptions of normality of the distribution were not verified. Post hoc multiple comparisons were made using the Steel–Dwass method. In addition, statistical analysis of nominal variables was performed with the chi-squared test.

Results

This study was carried out to examine the effects of *MGP* gene promoter polymorphisms (T-138C and G-7A) on the progression of VC in patients undergoing MHD. The T-138C and G-7A polymorphisms are located in the promoter region of the *MGP* gene (Fig. 2). Sequencing results of these polymorphisms are also shown in Fig. 2. The distribution of the T-138C genotype in this study was TT (35.1 %, $n = 47$), CT (52.2 %, $n = 70$) and CC (12.7 %, $n = 17$) (Fig. 3a). Similarly, the frequency of the G-7A genotype was GG (85.1 %, $n = 114$), GA (12.7 %, $n = 17$) and AA (2.2 %, $n = 3$) (Fig. 3b). We then compared the T-138C allele frequency of this study with that from the database of the genome-wide association study (GWAS); a chi-squared test showed no significant differences between them ($p = 0.73$, data not shown). In contrast, we could get no information on the G-7A allele frequency in GWAS. For that reason, we decided to place the primary focus on the analyses of the T-138C genotype.

Clinical characteristics of all patients of each genotype of T-138C are presented in Table 1. We found that the CC genotype was associated with significantly higher concentrations of high-density lipoprotein (HDL) cholesterol ($p = 0.03$).

Figure 4a shows the progression of the AACVS throughout the study (mean $R^2 = 0.87$), and Fig. 4b, c and d show the scores for the CC ($n = 17$), CT ($n = 70$) and TT ($n = 47$) genotypes, respectively. The dashed line shows the mean scores for all patients in each genotype group.

In order to investigate the effect of the T-138C genotype on the serum MGP concentration, we analyzed the MGP concentrations in the sera of MHD patients. There were no

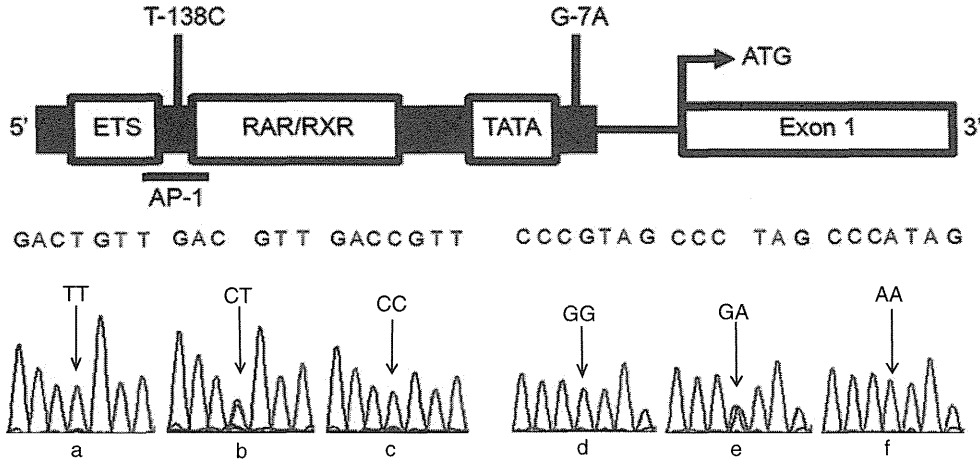

Fig. 2 DNA sequences of the polymorphic region in the MGP (T-138C, G-7A). **a** DNA sequence from individual homozygous for the TT genotype of T-138C. **b** heterozygous for the CT genotype of T-138C. **c** Homozygous for the CC genotype of T-138C. **d** DNA sequence from individual homozygous for the GG genotype of G-7A. **e** heterozygous for the GA genotype of G-7A. **f** homozygous for the AA genotype of G-7A. *ETS* Ets transcription factor family, *AP-1* activating protein-1, *RAR/RXR* retinoid A and X receptor, *TATA* TATA box

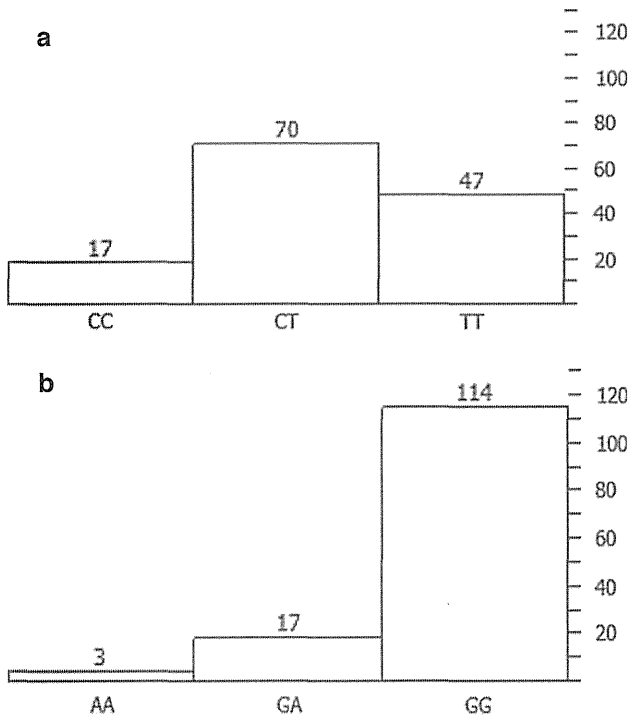

Fig. 3 The distribution of T-138C and G-7A genotype. **a** The distribution of the T-138C genotype ($n = 134$). **b** The distribution of the G-7A genotype ($n = 134$)

significant differences in the serum MGP concentration among the genotypes [CC: 22.57 (21.41, 28.43), CT: 25.10 (21.23, 26.87), TT: 25.01 (23.07, 26.45); unit: nmol/L, $p = 0.72$].

We compared the result of the slope value of the absolute AACVS plots as a linear function among the T-138C genotypes (Fig. 5a). The slope value for the CC genotype [53.00 (12.11, 254.90)] was significantly smaller than that for the CT genotype [319.85 (110.70, 647.80)] and TT genotype [261.00 (85.50, 626.56)] ($p = 0.003$, 0.03). Figure 5b shows the results of the comparison of the y-intercepts among the T-138C genotypes; there were no significant differences among them ($p = 0.52$). It is generally believed that the progression of VC at the beginning of MHD would contribute to the acceleration of VC and long-term survival of MHD patients [20]. Interestingly, however, our results indicate that the CC genotype of T-138C significantly contributes to the slowing of VC progression, regardless of differences in the VC volume at the beginning of MHD.

Multiple regression analysis by the best subset regression method between the progression speed of AACVS and related parameters revealed that CT/TT genotypes, greater age at the beginning of MHD, male sex, high levels of calcium × phosphate (Ca × P), low levels of HDL cholesterol, high levels of low-density lipoprotein (LDL) cholesterol, low levels of ferritin and non-use of angiotensin receptor blockers (ARBs) contributed to the progression of VC (Table 2).

Discussion

Although AAC is reported as a predictor for cardiovascular mortality in the general population, it is unknown whether this is also true in MHD patients. In addition, although many studies have focused on coronary calcification, there have been very few studies assessing the progression of AAC in MHD patients. A system for quantification of calcification was described by Kauppila et al. [21] in a subgroup of participants of the Framingham heart study. It relies on lateral lumbar radiographs and the calculation of the AAC score. Its predictive value for cardiovascular events and mortality was validated in the Framingham heart study [22, 23]. Recently, the AAC score was shown to correlate well with electron beam CT scores of the coronary arteries in MHD patients [24]. AAC may also be associated with all-cause and cardiovascular mortality in ESKD [25]. More recently, VC scores determined by MDCT were shown to be useful for evaluating the volume of VC [18]. For that reason, we used MDCT examinations for evaluation of the progression of VC in MHD patients.

The progression speed of VC differed among the MHD patients, and we hypothesized that MGP polymorphisms had some effect on this variation. Our study proved that MHD patients with the MGP T-138C CC genotype exhibited slower progression of VC than those with other genotypes. To our knowledge, this is the first study to reveal that the MGP T-138C polymorphism is closely linked to differences in the progression speed of VC among MHD patients.

MGP T-138C polymorphisms lie in the promoter region of the *MGP* gene, which is critical for the transcriptional activity. Farzaneh-Far et al. [13] previously showed that the −138C variant provides higher levels of MGP transcriptional activity in vascular smooth muscle cells. Therefore, our clinical data imply that the −138C allele increases MGP promoter activity in the arterial vessel and works more protectively against the progression of VC in MHD patients with the CC genotype. Furthermore, a previous study demonstrated that the −138C variant is associated with higher serum MGP levels (+30 %) [13]. On the other hand, the serum MGP level was not correlated with T-138C polymorphisms in another study [26]. Our results in this study also showed no relation between the MGP polymorphisms and serum MGP levels. Several reports have demonstrated that MGP expression was increased in atherosclerotic arteries [27, 28]. From in situ hybridization, it was shown that MGP mRNA transcription takes place in the arterial vessel wall, and is particularly upregulated in atherosclerotic arteries [27]. Thus, local MGP upregulation

Table 1 Clinical characteristics of all the patients of each genotype of T-138C

	Characteristic	CC (n = 17)	CT (n = 70)	TT (n = 47)	p value[a]
Basic	Age at the beginning of HD (years)	61 (44, 72)	57 (49, 69)	57 (50, 68)	0.90
	Age at the time of this study	62 (48, 74)	63 (53.8, 74)	60 (53, 70)	0.85
	Male % (n)	82.4 (14)	68.6 (48)	70.2 (33)	0.53
	Body mass index (kg/m^2)	21.6 (19.0, 24.2)	22.4 (20.4, 24.9)	22.6 (20.0, 23.9)	0.53
	HD duration (month)	26 (18, 39)	42 (23, 74)	41 (22, 77)	0.10
	Diabetes % (n)	23.5 (4)	47.1 (33)	40.4 (19)	0.20
Medications (po)	Statin % (n)	23.5 (4)	11.4 (8)	10.6 (5)	0.35
	Antihypertensives				
	Calcium channel blocker % (n)	13.3 (2)	30.0 (21)	36.2 (17)	0.17
	ACE inhibitor % (n)	0.0 (0)	1.4 (1)	2.1 (1)	0.82
	ARB % (n)	17.7 (3)	31.4 (22)	27.7 (13)	0.52
	Vitamin K % (n)	5.9 (1)	1.4 (1)	4.3 (2)	0.51
	Antiplatelet % (n)	29.4 (5)	37.1 (26)	31.9 (15)	0.76
	Warfarin % (n)	0.0 (0)	4.3 (3)	4.3 (2)	0.69
	Calcium carbonate % (n)	70.6 (12)	81.4 (57)	85.1 (40)	0.42
	Active vitamin D % (n)	82.4 (14)	60.0 (42)	57.5 (27)	0.17
	Sevelamar hydrochloride % (n)	17.7 (3)	27.1 (19)	23.4 (11)	0.70
	Cinacarcet % (n)	0.0 (0)	1.4 (1)	4.3 (2)	0.48
	Lanthanum carbonate % (n)	11.8 (2)	14.3 (10)	12.8 (6)	0.95
	Steroid % (n)	5.9 (1)	5.7 (4)	2.1 (1)	0.63
HD-related parameters	Kt/V	1.49 (1.41, 1.62)	1.46 (1.30, 1.67)	1.48 (1.33, 1.60)	0.80
	HD (hours)	4 (4, 4)	4 (4, 4)	4 (4, 4)	0.69
Laboratory data (blood)	Total protein (mg/dL)	6.3 (6.1, 6.5)	6.2 (5.9, 6.6)	6.2 (6.0, 6.6)	0.54
	Albumin (mg/dL)	3.6 (3.5, 3.9)	3.6 (3.4, 3.8)	3.7 (3.5, 3.8)	0.14
	Total cholesterol (mg/dL)	163 (136, 184)	154 (136, 180)	156 (139, 176)	0.97
	HDL cholesterol (mg/dL)	54 (40, 62)	42 (33, 51)	38 (32, 53)	0.03*
	LDL cholesterol (mg/dL)	67 (55, 104)	78 (67, 100)	78 (66, 97)	0.62
	Triglyceride (mg/dL)	123 (63, 156)	105 (70, 158)	119 (85, 223)	0.32
	Blood glucose (mg/dL)	128 (113, 151)	126 (102, 146)	125 (96, 151)	0.88
	HbA1c (%): only diabetic patients (n = 4:33:19)	5.7 (5.4, 8.3)	5.8 (5.5, 7.6)	6.2 (5.5, 6.7)	0.98
	GA (%): only diabetic patients (n = 4:33:19)	19.7 (17.2, 29.5)	19.5 (16.7, 23.6)	22.0 (20.3, 24.6)	0.12
	C-reactive protein (mg/dL)	0.1 (0.0, 0.2)	0.1 (0.0, 0.4)	0.1 (0.0, 0.2)	1.00
	Calcium (mg/dL)	9.0 (8.2, 9.5)	8.9 (8.6, 9.4)	9.1 (8.6, 9.7)	0.41
	Phosphate (mg/dL)	4.6 (3.8, 5.4)	4.9 (4.0, 5.6)	4.8 (4.2, 5.6)	0.46
	Calcium × phosphate	40.9 (32.0, 48.6)	43.4 (34.0, 49.6)	44.2 (36.9, 53.0)	0.30
	Intact-PTH (pg/mL)	75 (36, 105)	74 (39, 129)	63 (39, 145)	0.86
	Hemoglobin (g/dL)	11.2 (10.7, 11.7)	11.1 (10.5, 11.7)	10.9 (10.4, 11.8)	0.79
	Ferritin (ng/mL)	126 (94, 158)	132 (79, 192)	130 (55, 173)	0.64
	β2 microglobulin (mg/L)	23.9 (20.1, 26.0)	25.8 (22.0, 30.9)	25.8 (23.1, 30.6)	0.16
	Blood urea nitrogen (mg/dL)	64.8 (51.5, 81.9)	63.8 (56.5, 76.2)	69.1 (60.6, 80.0)	0.39
	Creatinine (mg/dL)	11.40 (9.33, 13.58)	11.73 (9.61, 13.39)	11.63 (10.22, 14.02)	0.70

Data are presented in % (n) for categorical variables, and as median (25th, 75th percentile) for continuous variables

We analyzed the MGP concentrations in the sera of 48 MHD patients (CC: n = 7, CT: n = 26, TT: n = 15) because of discontinuation of the kit from Biomedica. There were no significant differences in the serum MGP concentration among the genotypes (CC: 22.57 (21.41, 28.43), CT: 25.10 (21.23, 26.87), TT: 25.01 (23.07, 26.45), unit: nmol/L, p = 0.72)

ACE angiotensin-converting enzyme, *ARB* angiotensin receptor blocker, GA glycated albumin, *HD* hemodialysis, *HDL* high-density lipoprotein, *LDL* low-density lipoprotein *PTH* parathyroid hormone

* $p < 0.05$

[a] Chi-squared test was used for categorical variables, and Kruskal–Wallis tests were used for continuous variables

in arterial walls may be a central mechanism counteracting the progression of excessive VC. Furthermore, a recent study reported that gremlin, one of the bone morphogenetic protein (BMP) antagonists, binds to precursors of BMP and inhibits their function [29]. BMP is an osteoinductive factor expressed in atherosclerotic lesions and MGP is

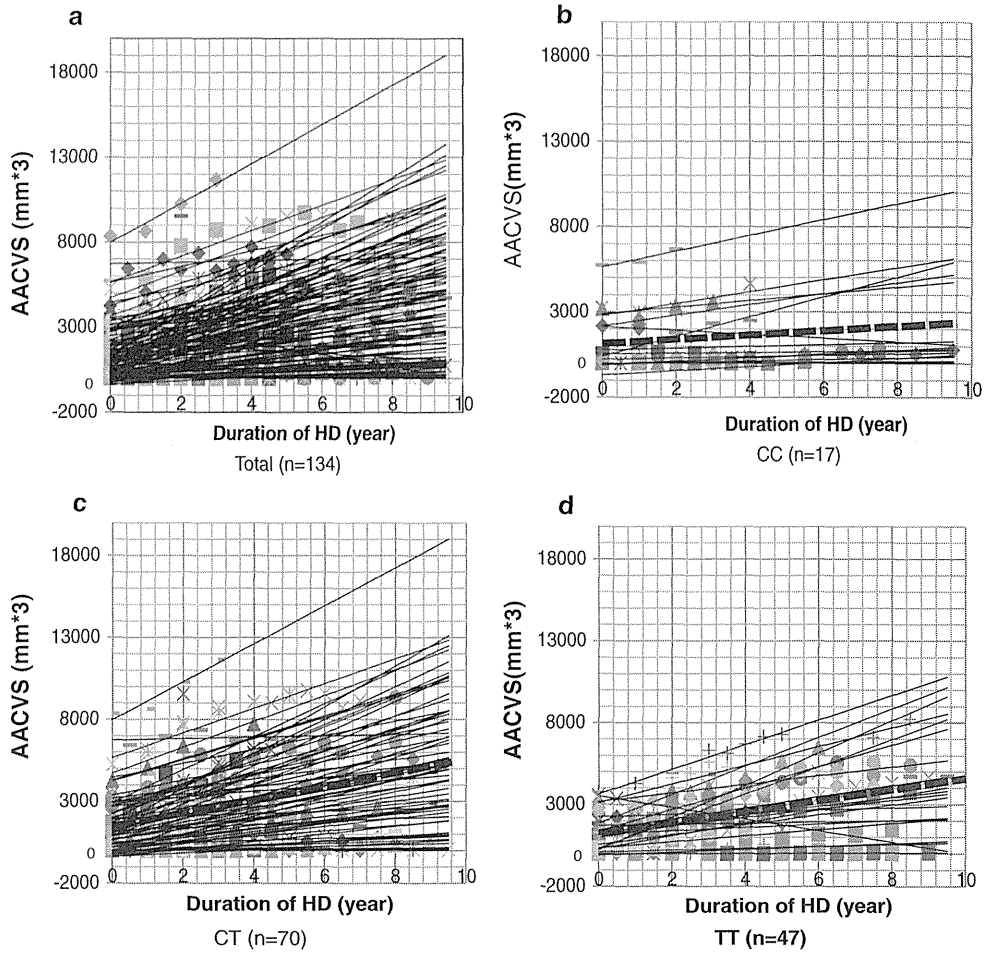

Fig. 4 Plots of the abdominal aortic calcium volume score (AACVS) as a linear function of each patients. **a** Plots of total patients (mean $R^2 = 0.87$). **b** Plots of only patients with the CC genotype of T-138C. **c** Plots of only patients with the CT genotype of T-138C. **d** Plots of only patients with the TT genotype of T-138C. The *dashed line* shows the mean scores for all patients in each genotype group

thought to be a BMP inhibitor. Therefore, the intracellular function to block BMP activation may be true of MGP and MGP may prevent arteries from calcification. Together with these findings, our study suggests that the CC genotype of T-138C may enhance the local activation of MGP independently of the serum MGP concentration, and may have the potential to inhibit VC in MHD patients.

We performed multiple regression analysis by the best subset regression method between the progression speed of VC and related parameters (Table 2), suggesting that the CC genotype of T-138C would function as a preventive factor for VC. Moreover, greater age at the beginning of MHD, high levels of Ca × P, low levels of HDL cholesterol, high levels of LDL cholesterol, and non-use of ARBs are all classic factors contributing to the progression of VC. With regard to gender, Yamada et al. [30] previously showed that the progression of AAC was negatively associated with the premenopausal status in women, which was considered to be due to female sex hormones. In our study, however, 34 of 39 (87.2 %) female participants were >50 years. Additionally, in our study, the CC genotype of T-138C was associated with higher concentrations of HDL cholesterol in the cross-sectional data (Table 1), and low levels of HDL cholesterol were significantly associated with progression of VC (Table 2). Yao et al. [31] previously reported in vitro that an increasing concentration of HDL cholesterol progressively enhanced expression of the activin-like kinase receptor 1 (ALK1) in human aortic endothelial cells, and that induction of ALK1 was associated with increased levels of MGP as determined by real-time PCR. This report supports our present data because high levels of HDL cholesterol may induce upregulation of focal MGP expression in the artery wall and subsequently halt the progression of VC. However, further investigations are needed to fully understand the mechanisms of regulation of HDL level in the CC genotype. Additionally, we tried taking the presence of diabetes, blood glucose and dialysis vintage (month) into the multiple regression analysis by the conventional model and the best subset regression method (stepwise method). These parameters were found not to influence the progression speed of VC in our analysis. Collectively, the most important finding in our study was that the MGP genotype was an invariable parameter related to the longitudinal VC progression.

There were several limitations to our study. The sample size of the study population was relatively small for a genetic association study. Therefore, further studies with a larger

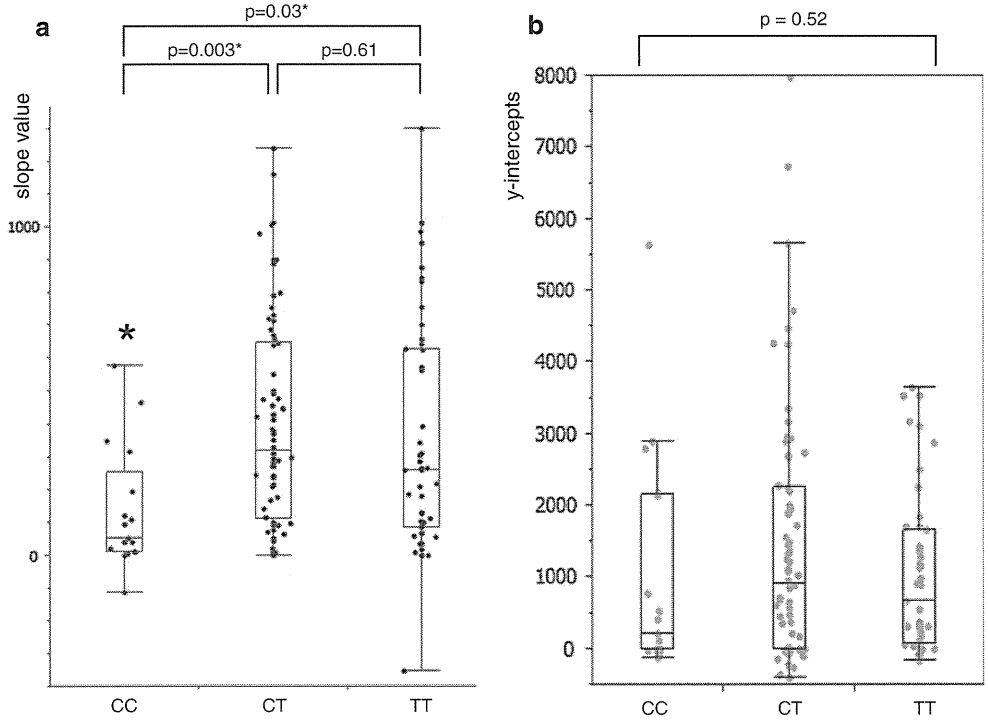

Fig. 5 The comparison of the progression speed of vascular calcification among the T-138C genotype. **a** The differences of the progression speed of the abdominal aortic calcium volume score (AACVS). **b** The comparison result of the vascular calcification (VC) at the beginning of HD (*y*-intercepts). Both were analyzed by Kruskal–Wallis test and Steel–Dwass test

Table 2 Multiple regression analysis between the progression speed of AACVS and related parameters

Covariate	Coefficient	95 % CI	Standardized β	*p* value
CT/TT genotype of T-138C	87.06	(19.04, 155.07)	0.25	0.01*
Age at the beginning of HD (years)	9.10	(5.14, 13,07)	0.38	<0.001*
Female sex	−73.30	(−127.38, −19.22)	−0.20	0.008*
Ca × P	9.15	(4.61, 13.70)	0.33	<0.001*
HDL cholesterol (mg/dL)	−3.44	(−6.60, −0.28)	−0.16	0.03*
LDL cholesterol (mg/dL)	3.09	(1.10, 5.07)	0.23	0.003*
Ferritin (ng/mL)	−0.65	(−1.13, −0.16)	−0.20	0.01*
ARBs	−63.70	(−117.61, −9.78)	−0.18	0.02*

$n = 134$, $R^2 = 0.34$, $F = 7.1936$, $p < 0.001$, Durbin–Watson ratio 1.9365483

ARBs angiotensin receptor blockers, *Ca* × *P* calcium × phosphate, *HD* hemodialysis, *HDL* high-density lipoprotein, *LDL* low-density lipoprotein

* $p < 0.05$

number of subjects in different groups with different characteristics are needed. We need to continue this study prospectively in order to investigate relationships to cardiovascular events and long-term mortality. In addition, large-scale follow-up studies with high-risk CKD patients would enhance and vary the information about the genetic background.

Conclusions

This study emphasizes that MGP T-138C polymorphism is closely linked to the progression speed of VC in MHD patients. VC is very common in MHD patients and is a strong predictor of cardiovascular disease and all-cause mortality. In particular, accelerated progressive VC strongly deteriorates the prognosis of MHD patients. We propose here that the genotype of the *MGP* gene might be a genomic biomarker that is predictive of VC progression. Furthermore, this inalterable biomarker may be helpful for disease detection and classification, treatment response prediction, treatment efficacy, and prognosis.

Acknowledgments The authors thank A. Sakurai, T. Sasaki, and S. Hayashi for their technical support. This study was supported in part

by a Grant-in-Aid for Diabetic Nephropathy, Research from the Ministry of Health, Labour and Welfare of Japan and a grant from The Kidney Foundation, Japan (JKFB10-28 and JKF10-2).

Conflict of interest The authors have declared that no conflict of interest exists.

References

1. Raggi P, Boulay A, Chasan-Taber S, Amin N, Dillon M, Burke SK, et al. Cardiac calcification in adult hemodialysis patients. A link between end-stage renal disease and cardiovascular disease? J Am Coll Cardiol. 2002;39:695–701.
2. Goodman WG, Goldin J, Kuizon BD, Yoon C, Gales B, Sider D, et al. Coronary-artery calcification in young adults with end-stage renal disease who are undergoing dialysis. N Engl J Med. 2000;342:1478–83.
3. Block GA, Spiegel DM, Ehrlich J, Mehta R, Lindbergh J, Dreisbach A, et al. Effects of sevelamer and calcium on coronary artery calcification in patients new to hemodialysis. Kidney Int. 2005;68:1815–24.
4. Blacher J, Guerin AP, Pannier B, Marchais SJ, London GM. Arterial calcifications, arterial stiffness, and cardiovascular risk in end-stage renal disease. Hypertension. 2001;38:938–42.
5. London GM, Guérin AP, Marchais SJ, Métivier F, Pannier B, Adda H. Arterial media calcification in end-stage renal disease: impact on all-cause and cardiovascular mortality. Nephrol Dial Transplant. 2003;18:1731–40.
6. Maréchal C, Schlieper G, Nguyen P, Krüger T, Coche E, Robert A, et al. Serum fetuin-A levels are associated with vascular calcifications and predict cardiovascular events in renal transplant recipients. Clin J Am Soc Nephrol. 2011;6:974–85.
7. Price PA, Otsuka AS, Poser JW, Kristaponis J, Raman N. Characterization of a gamma-carboxyglutamic acid-containing protein from bone. Proc Natl Acad Sci USA. 1976;73:1447–51.
8. Covic A, Kanbay M, Voroneanu L, Turgut F, Serban DN, Serban IL, et al. Vascular calcification in chronic kidney disease. Clin Sci (Lond). 2010;119:111–21.
9. Luo G, Ducy P, McKee MD, Pinero GJ, Loyer E, Behringer RR, et al. Spontaneous calcification of arteries and cartilage in mice lacking matrix GLA protein. Nature. 1997;386:78–81.
10. Moe SM, Chen NX. Pathophysiology of vascular calcification in chronic kidney disease. Circ Res. 2004;95:560–7.
11. Braam LA, Dissel P, Gijsbers BL, Spronk HM, Hamulyák K, Soute BA, et al. Assay for human matrix gla protein in serum: potential applications in the cardiovascular field. Arterioscler Thromb Vasc Biol. 2000;20:1257–61.
12. Herrmann SM, Whatling C, Brand E, Nicaud V, Gariepy J, Simon A, et al. Polymorphisms of the human matrix gla protein (MGP) gene, vascular calcification, and myocardial infarction. Arterioscler Thromb Vasc Biol. 2000;20:2386–93.
13. Farzaneh-Far A, Davies JD, Braam LA, Spronk HM, Proudfoot D, Chan SW, et al. A polymorphism of the human matrix gamma-carboxyglutamic acid protein promoter alters binding of an activating protein-1 complex and is associated with altered transcription and serum levels. J Biol Chem. 2001;276:32466–73.
14. Brancaccio D, Biondi ML, Gallieni M, Turri O, Galassi A, Cecchini F, et al. Matrix GLA protein gene polymorphisms: clinical correlates and cardiovascular mortality in chronic kidney disease patients. Am J Nephrol. 2005;25:548–52.
15. Crosier MD, Booth SL, Peter I, Dawson-Hughes B, Price PA, O'Donnell CJ, et al. Matrix Gla protein polymorphisms are associated with coronary artery calcification in men. J Nutr Sci Vitaminol (Tokyo). 2009;55:59–65.
16. Schurgers LJ, Teunissen KJ, Knapen MH, Geusens P, van der Heijde D, Kwaijtaal M, et al. Characteristics and performance of an immunosorbent assay for human matrix Gla-protein. Clin Chim Acta. 2005;351:131–8.
17. Callister TQ, Cooil B, Raya SP, Lippolis NJ, Russo DJ, Raggi P. Coronary artery disease: improved reproducibility of calcium scoring with an electron-beam CT volumetric method. Radiology. 1998;208:807–14.
18. Floege J, Raggi P, Block GA, Torres PU, Csiky B, Naso A, et al. Study design and subject baseline characteristics in the ADVANCE Study: effects of cinacalcet on vascular calcification in haemodialysis patients. Nephrol Dial Transplant. 2010;25:1916–23.
19. Raggi P, Callister TQ, Shaw LJ. Progression of coronary artery calcium and risk of first myocardial infarction in patients receiving cholesterol-lowering therapy. Arterioscler Thromb Vasc Biol. 2004;24:1272–7.
20. Block GA, Raggi P, Bellasi A, Kooienga L, Spiegel DM. Mortality effect of coronary calcification and phosphate binder choice in incident hemodialysis patients. Kidney Int. 2007;71:438–41.
21. Kauppila LI, Polak JF, Cupples LA, Hannan MT, Kiel DP, Wilson PW. New indices to classify location, severity and progression of calcific lesions in the abdominal aorta: a 25-year follow-up study. Atherosclerosis. 1997;132:245–50.
22. Wilson PW, Kauppila LI, O'Donnell CJ, Kiel DP, Hannan M, Polak JM, et al. Abdominal aortic calcific deposits are an important predictor of vascular morbidity and mortality. Circulation. 2001;103:1529–34.
23. Walsh CR, Cupples LA, Levy D, Kiel DP, Hannan M, Wilson PW, et al. Abdominal aortic calcific deposits are associated with increased risk for congestive heart failure: the Framingham Heart Study. Am Heart J. 2002;144:733–9.
24. Bellasi A, Ferramosca E, Muntner P, Ratti C, Wildman RP, Block GA, et al. Correlation of simple imaging tests and coronary artery calcium measured by computed tomography in hemodialysis patients. Kidney Int. 2006;70:1623–8.
25. Okuno S, Ishimura E, Kitatani K, Fujino Y, Kohno K, Maeno Y, et al. Presence of abdominal aortic calcification is significantly associated with all-cause and cardiovascular mortality in maintenance hemodialysis patients. Am J Kidney Dis. 2007;49:417–25.
26. Karsli Ceppioglu S, Yurdun T, Canbakan M. Assessment of matrix gla protein, klotho gene polymorphisms, and oxidative stress in chronic kidney disease. Ren Fail. 2011;33:866–74.
27. Shanahan CM, Cary NR, Metcalfe JC, Weissberg PL. High expression of genes for calcification-regulating proteins in human atherosclerotic plaques. J Clin Invest. 1994;93:2393–402.
28. Dhore CR, Cleutjens JP, Lutgens E, Cleutjens KB, Geusens PP, Kitslaar PJ, et al. Differential expression of bone matrix regulatory proteins in human atherosclerotic plaques. Arterioscler Thromb Vasc Biol. 2001;21:1998–2003.
29. Sun J, Zhuang FF, Mullersman JE, Chen H, Robertson EJ, Warburton D, et al. BMP4 activation and secretion are negatively regulated by an intracellular gremlin-BMP4 interaction. J Biol Chem. 2006;281:29349–56.
30. Yamada K, Fujimoto S, Nishiura R, Komatsu H, Tatsumoto M, Sato Y, et al. Risk factors of the progression of abdominal aortic calcification in patients on chronic haemodialysis. Nephrol Dial Transplant. 2007;22:2032–7.
31. Yao Y, Shao ES, Jumabay M, Shahbazian A, Ji S, Boström KI. High-density lipoproteins affect endothelial BMP-signaling by modulating expression of the activin-like kinase receptor 1 and 2. Arterioscler Thromb Vasc Biol. 2008;28:2266–74.

Anal Bioanal Chem (2012) 404:3101–3109
DOI 10.1007/s00216-012-6412-x

ORIGINAL PAPER

Metabolic profiling reveals new serum biomarkers for differentiating diabetic nephropathy

Akiyoshi Hirayama · Eitaro Nakashima · Masahiro Sugimoto · Shin-ichi Akiyama · Waichi Sato · Shoichi Maruyama · Seiichi Matsuo · Masaru Tomita · Yukio Yuzawa · Tomoyoshi Soga

Received: 2 July 2012 / Revised: 4 September 2012 / Accepted: 5 September 2012 / Published online: 29 September 2012

Abstract Capillary electrophoresis coupled with time-of-flight mass spectrometry was used to explore new serum biomarkers with high sensitivity and specificity for diabetic nephropathy (DN) diagnosis, through comprehensive analysis of serum metabolites with 78 diabetic patients. Multivariate analyses were used for identification of marker candidates and development of discriminative models. Of the 289 profiled metabolites, orthogonal partial least-squares discriminant analysis identified 19 metabolites that could distinguish between DN with macroalbuminuria and diabetic patients without albuminuria. These identified metabolites included creatinine, aspartic acid, γ-butyrobetaine, citrulline, symmetric dimethylarginine (SDMA), kynurenine, azelaic acid, and galactaric acid. Significant correlations between all these metabolites and urinary albumin-to-creatinine ratios ($p<0.009$, Spearman's rank test) were observed. When five metabolites (including γ-butyrobetaine, SDMA, azelaic acid and two unknowns) were selected from 19 metabolites and applied for multiple logistic regression model, AUC value for diagnosing DN was 0.927 using the whole dataset, and 0.880 in a cross-validation test. In addition, when four known metabolites (aspartic acid, SDMA, azelaic acid and galactaric acid) were applied, the resulting AUC was still high at 0.844 with the whole dataset and 0.792 with cross-validation. Combination of serum metabolomics with multivariate analyses enabled accurate discrimination of DN patients. The results suggest that capillary electrophoresis-mass spectrometry based metabolome analysis could be used for DN diagnosis.

Keywords Diabetic nephropathy · Capillary electrophoresis-mass spectrometry · Metabolome · Biomarker · Multiple logistic regression · Orthogonal partial least-squares discriminant analysis

A. Hirayama · M. Sugimoto · M. Tomita · T. Soga (✉)
Institute for Advanced Biosciences, Keio University,
246-2 Mizukami, Kakuganji,
Tsuruoka, Yamagata 997-0052, Japan
e-mail: soga@sfc.keio.ac.jp

E. Nakashima
Japan Labour Health and Welfare Organization Chubu Rosai Hospital,
1-10-6 Koumei-cho, Minato-ku,
Nagoya, Aichi 455-8530, Japan

E. Nakashima
Department of Endocrinology and Diabetes, Nagoya University Graduate School of Medicine,
65 Tsurumai-cho, Showa-ku,
Nagoya, Aichi 466-8550, Japan

M. Sugimoto
Medical Innovation Center, Kyoto University Graduate School of Medicine,
Yoshida Konoe, Sakyo-ku,
Kyoto 606-8501, Japan

S.-i. Akiyama · W. Sato · S. Maruyama · S. Matsuo · Y. Yuzawa
Department of Nephrology of Internal Medicine, Nagoya University Graduate School of Medicine,
65 Tsurumai-cho, Showa-ku,
Nagoya, Aichi 466-8550, Japan

Introduction

Diabetic nephropathy (DN) is one of the major complications of diabetes mellitus (DM) and has become the most prevalent cause of end-stage renal disease worldwide [1]. DN is also one of the most significant long-term diseases in terms of morbidity and mortality for individuals with diabetes [2]. Recent

studies have shown that several interventions can slow the progression of DN, and their impact is greater if they are started at an early stage of the development of nephropathy [3]. Although renal biopsy is the most accurate diagnostic method for DN, routine renal biopsies are not acceptable in current clinical practice because of their invasiveness. Microalbuminuria is an alternative, non-invasive marker that can be used for DN risk assessment, and the urinary albumin-to-creatinine ratio (UACR) on first-void urine sample is recommended for DN screening. However, large prospective studies have revealed poor accuracy of this marker, even though urine samples are collected two or three times a day to normalize day-to-day variation [4]. Therefore, identifying reliable and versatile biomarkers for risk assessment of DN is important.

Mass spectrometry-based urinary proteomics is used for biomarker discoveries of DN. Dihazi et al. used surface-enhanced laser desorption/ionization time-of-flight mass spectrometry to identify three urinary proteins that differentiated patients with DN from patients with type 2 DM without nephropathy, patients with type 2 DM with micro- or macroalbuminuria, patients with proteinuria caused by non-diabetic renal disease, and healthy controls [5]. Mischak et al. profiled urinary polypeptides using capillary electrophoresis-mass spectrometry (CE-MS) and found that the MS patterns could be used to differentiate type 2 DM from healthy controls [6]. However, urinary protein markers sometimes show a wider variation than blood samples. Thus, it is necessary to discover biomarkers with small diurnal variations.

Metabolomics is the comprehensive analysis of low weight molecules in a sample, and has become a powerful tool in the biomarker discovery field. Nuclear magnetic resonance [7], gas chromatography-mass spectrometry [8], liquid chromatography-mass spectrometry (LC-MS; [9]), and CE-MS [10–12] are currently used for metabolomics. Targeted profiling, that is, detection of only a few sets of metabolites, has been used to discover biomarkers for DN. Xia et al. analyzed six intermediate metabolites of the purine degradation pathway in plasma from patients with non-DN and DN using LC with or without MS [13]. They found that adenosine, inosine, uric acid, and xanthine were useful biomarkers for monitoring DM progression. Jiang et al. used LC-tandem mass spectrometry to simultaneously quantify eight aminothiols in the homocysteine metabolic cycle in plasma and found two sulfur-containing metabolites, *S*-adenosylmethionine and *S*-adenosylhomocysteine, as potential biomarkers for DM and DN [14].

Compared to targeted profiling, comprehensive metabolome analysis of all metabolites in the given sample is a more powerful technique. Zhang et al. used non-targeted LC-MS to detect potential biomarker candidates of DN and type 2 DM, and observed significant differences in the serum levels of leucine, dihydrosphingosine, and phytosphingosine [15]. However, there are few published comprehensive metabolome profiles of DN.

Recently, we developed a non-targeted CE-MS-based metabolome profiling technique [11, 16] and applied it to biomarker discovery for acetaminophen-induced hepatotoxicity in mice [11] and several types of cancer-specific profiles in human saliva [12]. In the present study, we used CE-MS to identify serum metabolite biomarkers for DN diagnosis. Furthermore, classification models incorporating multiple biomarkers were constructed for discriminating DN from non-DN.

Materials and methods

Sample collection and metabolite extraction

All experiments were conducted in accordance with study protocol approved by the Institutional Ethics Committee of Chubu Rosai Hospital. Informed consent was obtained from all patients according to the Declaration of Helsinki as revised in 2000. Serum samples from 78 type 2 DM patients were collected and classified into the following three groups: DM group without nephropathy and albuminuria (non-DN, UACR<30 mg/g, n=20), early DN group with microalbuminuria (micro-DN, 30<UACR<300 mg/g, n=32), and overt DN group with macroalbuminuria (macro-DN, UACR>300 mg/g, n=26). All serum samples were stored at −80 °C.

To extract metabolites, the frozen sera samples were thawed and 100 μl aliquots were put into 900 μl of methanol that contained internal standards (20 μmol/l each of methionine sulfone and camphor 10-sulfonic acid). The internal standards were used to normalize the extraction efficiency of metabolites during sample preparation for both cationic (methionine sulfone) and anionic (camphor 10-sulfonic acid) metabolite analysis. The solutions were mixed well and then 400 μl of Milli-Q water and 1 ml of chloroform were added, followed by centrifugation at 4,600×*g* for 5 min at 4 °C. The aqueous layer was transferred to a 5-kDa cutoff centrifugal filter tube (Millipore, Billerica, MA, USA) to remove large molecules. The filtrate was centrifugally concentrated at 35 °C and reconstituted with 50 μl of Milli-Q water that contained reference compounds (200 μmol/l each of 3-aminopyrrolidine and trimesic acid) immediately before CE-TOFMS analysis. These reference compounds were added to eliminate the variation in migration time of individual peaks in electropherogram among multiple datasets.

Reagents

Methionine sulfone (internal standard) was purchased from Alfa Aesar (Ward Hill, MA), and hexakis-(2,2-difluoroethoxy)-phosphazene (Hexakis) from SynQuest

Laboratories (Alachua, FL). All other reagents were obtained from Sigma-Aldrich (St. Louis, MO) or Wako Pure Chemicals Industries Ltd. (Osaka, Japan). All chemicals used were of analytical or reagent grade. Water was purified with a Milli-Q purification system (Millipore, Billerica, MA).

Instruments

All CE-electrospray ionization (ESI)-TOFMS experiments were performed using an Agilent CE capillary electrophoresis system (Agilent Technologies, Waldbronn, Germany), an Agilent G3250AA LC/MSD TOF system (Agilent Technologies, Palo Alto, CA, USA), an Agilent 1100 series isocratic HPLC pump, a G1603A Agilent CE-MS adapter kit, and a G1607A Agilent CE-ESI-MS sprayer kit. The CE-MS adapter kit included a capillary cassette, which facilitated thermostating of the capillary, and the CE-ESI-MS sprayer kit, which simplified coupling of the CE system with the MS system, was equipped with an electrospray source. For system control and data acquisition, G2201AA Agilent Chemstation software was used for CE, and Agilent TOF (Analyst QS) software was used for TOFMS. The original Agilent SST316Ti stainless steel (Fe/Cr/Ni/Mo/Ti; 68:18:11:2:1) ESI needle was replaced with a platinum needle for anion analysis [17]. The resolution of the TOFMS instrument used in this study is higher than 3,000 at *m/z* 100 with high mass accuracy (<3 ppm).

CE-TOFMS analysis of cationic metabolites

CE-TOFMS analysis of cationic metabolites was performed as described previously [10]. Cationic metabolites were separated in a fused-silica capillary (50 μm i.d. × 100 cm total length) filled with 1 mol/l formic acid as the reference electrolyte. The sample solution was injected at 5 kPa for 3 s (approximately 3 nl), and a positive voltage of 30 kV was applied. The capillary and sample trays were maintained at 20 °C and <5 °C, respectively. The sheath liquid was methanol/water (50 %*v*/*v*) containing 0.1 μmol/l Hexakis and was delivered at 10 μl/min. ESI-TOFMS was operated in positive ion mode. The capillary voltage was set at 4 kV, and the nitrogen gas (heater temperature 300 °C) flow rate was set at 10 l/min. In TOFMS, the fragmenter voltage, skimmer voltage, and octapole radio frequency voltage were set at 75, 50, and 125 V, respectively. An automatic recalibration function was performed using the following masses of two reference standards: [^{13}C isotopic ion of the protonated methanol dimer $(2MeOH + H)]^+$, *m/z* 66.06306; and [protonated Hexakis $(M + H)]^+$, *m/z* 622.02896. Mass spectra were acquired at a rate of 1.5 cycles per second from *m/z* 50 to 1000.

CE-TOFMS analysis of anionic metabolites

The CE-TOFMS analysis of anionic metabolites was performed as described previously [17]. Anionic metabolites were separated in a commercially available COSMO(+) capillary, which was chemically coated with a cationic polymer. Ammonium acetate solution (50 mmol/l, pH 8.5) was used as the electrolyte for CE separation. The sample solution was injected at 5 kPa for 30 s (approximately 30 nl) and a voltage of −30 kV was applied. Ammonium acetate (5 mmol/l) in methanol/water (50 %*v*/*v*) containing 0.1 μmol/l Hexakis was delivered as the sheath liquid at 10 μl/min. ESI-TOFMS was operated in negative ion mode. The capillary voltage was set at 3.5 kV. In TOFMS, the fragmenter voltage, skimmer voltage, and octapole radio frequency voltage were set at 100, 50, and 200 V, respectively. An automatic recalibration function was performed using the following masses of two reference standards: [^{13}C isotopic ion of deprotonated acetic acid dimer $(2CH_3COOH-H)]^-$, *m/z* 120.03834; and [Hexakis + deprotonated acetic acid $(M + CH_3COOH-H)]^-$, *m/z* 680.03554. Mass spectra were acquired at a rate of 1.5 cycles per second from *m/z* 50 to 1,000.

Data processing

The raw data were processed using our proprietary software (MasterHands) [10, 12]. The overall data processing flow consisted of noise filtering, baseline correction, peak detection, and integration of the peak areas from 0.02*m/z*-wide sections of the electropherograms. Subsequently, the accurate *m/z* of each peak was calculated by Gaussian curve fitting in the *m/z* domain, and the migration times were normalized to match the detected peaks among the multiple datasets. The peaks were identified by matching *m/z* values and normalized migration times of corresponding authentic standard compounds. Processed peak lists were exported for further statistical analysis.

Statistical analysis

The relative ratio of the detected peak area to that of the internal standard was used to eliminate systematic bias derived from injection volume variance and MS sensitivity. Data were analyzed with GraphPad Prism 5.0 (GraphPad Software, Inc., San Diego, CA, USA) for statistical tests. The Kruskal–Wallis test and Dunn's post test were used to assess the statistical significance of differences among non-DN, micro-DN and macro-DN samples. The Spearman's rank correlation test was used to calculate correlations among UACR, eGFR, and the relative ratios of peak areas of the metabolites. Multiple logistic regression (MLR) models were developed to discriminate non-DN and DN cohorts. Biomarker metabolites for these models were selected in

two procedures. First, normalized data were subjected to orthogonal partial least-squares discriminant analysis (OPLS-DA) using SIMCA-P + software (Version 12.0, Umetrics, Umeå, Sweden), and a model was built and used to identify marker metabolites that accounted for differentiation of non-DN and macro-DN cohorts. Next, a stepwise variable selection method (forward and backward selection) was conducted with a threshold of $p<0.25$ for adding and eliminating features using JMP 8.0 (SAS Institute Inc., Cary, NC, USA). The generalization ability of the developed MLR model was evaluated using cross-validation methods. Tenfold cross-validation was conducted 20 times with different random seeds using WEKA (ver. 3.6.1, The University of Waikato, Hamilton, New Zealand) to split the datasets into training and validation data [18]. Bootstrap analysis was also conducted to estimate the optimistic bias in the given datasets. Two hundred replicates, including the same number of patients, were computationally generated with a random selection of individuals, this permitted redundant selection, and MLR models were developed and cross-validation tests were conducted on each generated dataset.

Results

Metabolome analysis of serum samples obtained from non-DN and DN patients

Serum metabolome profiles of 78 patients in three successive stages of DN were collected using a single standard protocol [non-DN (n=20), micro-DN (n=32) and macro-DN (n=26)] and analyzed. Age distribution, gender and other clinical characteristics are listed in Table 1. The ages in the micro-DN and macro-DN groups were slightly higher than in the non-DN group (p=0.0226). The macro-DN group had significantly higher creatinine contents and lower estimated glomerular filtration rates (eGFR) than the other groups ($p<0.0001$), while no significant difference was seen between the non-DN and micro-DN groups. The macro-DN group also showed significantly higher triglycerides and systolic blood pressure (SBP) compared with the non-DN group (p=0.0172 and 0.0083, respectively). The other clinical parameters showed no significant difference among all groups ($p>0.05$).

On average, 4400 peaks were detected from each serum sample with CE-TOFMS. After eliminating redundant peaks, such as noise, fragments and adduct ions, 289 metabolites remained. Using this dataset, we firstly performed principal component analysis (PCA), but the resultant score plots of the PCA showed no unequivocal stage-specific clusters (data not shown). Next, OPLS-DA was performed to discriminate between DN patients (micro-DN and macro-DN) and non-DN patients based on the profiled metabolites. The OPLS-DA model demonstrated satisfactory separation between non-DN and micro-DN patients (Fig. 1a) using one predictive component and one orthogonal component (R^2X_{cum}=0.21, R^2Y_{cum}=0.676, $Q_{cum}{}^2$=0.179), and clear separation between non-DN and macro-DN patients (Fig. 1b) using one predictive component and three orthogonal components (R^2X_{cum}=0.353, R^2Y_{cum}=0.946, $Q_{cum}{}^2$=0.599). These results indicate that serum metabolome profile can be used to distinguish DN patients from non-DN patients.

The resultant S plot of the developed OPLS-DA model between non-DN and macro-DN patients identified 19 metabolites (Table 2) that were highly correlated in the separation of the groups (|p(corr)|>0.5). Of these, we were able to assign metabolite identities to eight metabolites by matching their m/z values and migration times with those of standard reagents. These metabolites were creatinine, aspartic acid, γ-butyrobetaine, citrulline, symmetric dimethylarginine (SDMA), kynurenine, azelaic acid, and galactaric acid. The composition formulae of the other metabolites were calculated based on their isotope distribution patterns as follows: $C_5H_8N_2O_2$ [metabolite ID (MID) 17], $C_9H_{17}NO$ (MID 51), $C_9H_{19}NO$ (MID 52), $C_2H_4N_2O_3$ (MID 158), and $C_6H_6N_4O$ (MID 202). Only the m/z values of the other metabolites are listed in Table 2 because of insufficient isotope peak size. The AUC values of MID 202 (0.765, 95 % CI); 0.649–0.880, $p=4.47\times10^{-4}$) gave the best discriminating ability among these markers (Table 3).

Correlation between biomarker candidates and clinical parameters

Correlation analysis between these 19 serum biomarker candidates and currently available clinical parameters showed all candidate metabolites were significantly correlated with UACR ($p<0.009$) (Table 4). The correlation coefficients for creatinine (r=0.5701), aspartic acid (r=0.4993), γ-butyrobetaine (r=0.4942), citrulline (r=0.4300), SDMA (r=0.4820), kynurenine (r=0.5351), MID 17 (r=0.4968), MID 97 (r=0.5223), MID 152 (r=0.5336), MID 158 (r=0.4980), and MID 202 (r=0.6352) were positively correlated with UACR. Those of azelaic acid (r=–0.5210), galactaric acid (r=–0.4596), MID 51 (r=–0.4728), MID 52 (r=–0.4871), MID 96 (r=–0.3085), MID 114 (r=–0.3638), MID 127 (r=–0.2961), and MID 134 (r=–0.3669) were negatively correlated. Furthermore, 15 of 19 metabolites were significantly correlated with eGFR ($p<0.035$). The correlation coefficients of creatinine (r=–0.8832), aspartic acid (r=–0.3912), γ-butyrobetaine (r=–0.6492), citrulline (r=–0.6531), SDMA (r=–0.7111), kynurenine (r=–0.5627), MID 17 (r=–0.5808), MID 97 (r=–0.7651), MID 152 (r=–0.7687), MID 158 (r=–0.6302), and MID

Table 1 Clinical characteristics of diabetic nephropathy patients

	Non-DN	Micro-DN	Macro-DN	*p* value
Number	20	32	26	
Male/Female	9/11	22/10	17/9	
Age (years)	57.5±12.9	66.6±9.2[a]	67.3±8.7[a]	0.0226
BMI (kg/m^2)	26.9±5.0	24.6±3.4 (1)	24.8±3.0	0.3074
HbA_{1c} (%)	6.8±1.0	7.2±1.1	6.8±0.7	0.3931
UACR (mg/g)	12.1±6.7	103.9±77.8[a]	1055.3±741.3[a, b]	<0.0001
Creatinine (enzymatic, mg/dL)	0.71±0.18	0.84±0.28	1.39±0.66[a,b]	<0.0001
Triglycerides (mg/dL)	134.6±131.5	133.5±55.2	179.7±110.3[a] (3)	0.0172
Cholesterol (mg/dL)	190.4±53.5 (2)	198.5±25.7 (2)	218.0±41.9 (1)	0.0838
HDL cholesterol (mg/dL)	56.3±18.9	50.9±14.6	52.9±21.1 (1)	0.5011
LDL cholesterol (mg/dL)	120.4±31.7	120.5±26.2 (1)	125.8±34.1 (1)	0.8421
Systolic BP (mmHg)	132±21	143±23	152±22[a]	0.0083
Diastolic BP (mmHg)	74±13	79±14	81±10	0.0711
eGFR (mL/min/1.73 m^2)	81.9±24.0	70.5±21.9	47.2±25.6[a,b]	<0.0001
Medication (number)				
Diabetic drug	17	27	25	
Hypolipidemic drug	10	16	14	
Antihypertensive drug	10	19	22	

The number in parentheses indicates the number of patients for which clinical values were missing. The *p* values were calculated using the data from the patients without missing values. Data are means±SD

[a]Significantly different compared to non-DN group

[b]Significantly different compared to micro-DN group

202 (r=–0.7455) showed negative correlation with eGFR. This indicates that they were positively associated with renal dysfunction. By contrast, those of azelaic acid (r=0.3739), galactaric acid (r=0.4152), MID 51 (r=0.2204), and MID 134 (r=0.2397) showed positive correlation with eGFR.

MLR model development

For the discrimination of DN (micro-DN and macro-DN) from non-DN patients, we developed a MLR model. Of the 19 biomarker candidates, γ-butyrobetaine, SDMA, azelaic acid, MID 114, and MID 127 were selected by stepwise feature selection as MLR variables. The developed model yielded high AUC values (0.927, 95 % CI, 0.870–0.983, p< 0.0001, Fig. 2a). The model also yielded high AUC values (±SD; 0.880±8.62×10^{-3}) in the cross-validation test. In a bootstrap test, the AUC values were 0.946±0.0262 and 0.895±0.0364 for training and cross-validation, respectively. To evaluate only the eight identified metabolites, we independently developed a MLR model. Stepwise feature selection selected aspartic acid, SDMA, azelaic acid, and galactaric acid as MLR variables. This MLR model also yielded high AUC values (0.844, 95 % CI, 0.754–0.934, p<0.0001, Fig. 2b), although it performed slightly worse than the model with all metabolites, including unknown peaks. This model also yielded high AUC values (±SD;

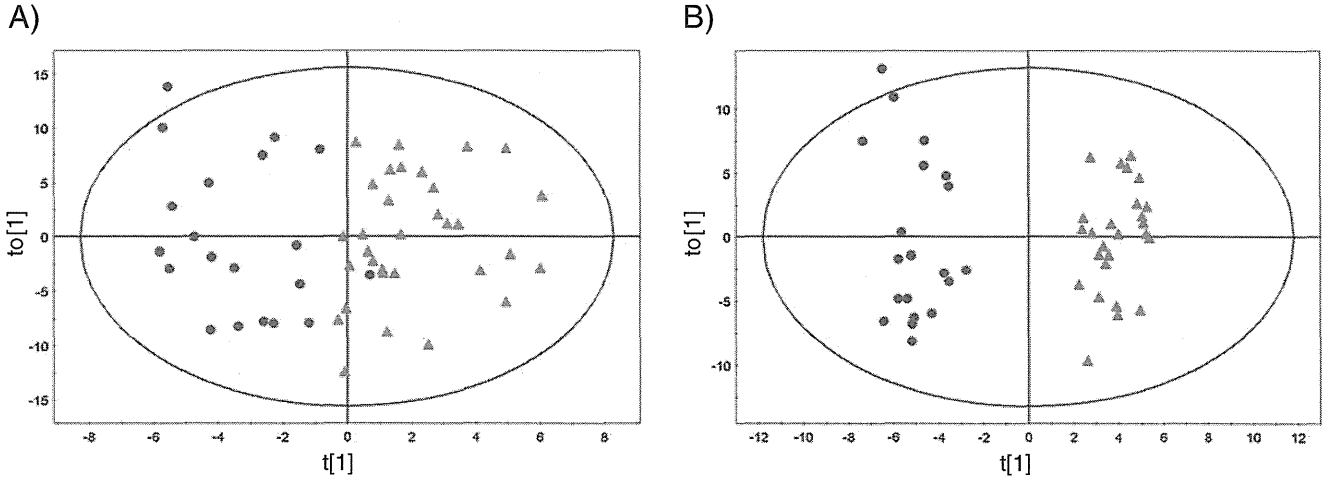

Fig. 1 OPLS-DA based on comprehensive metabolites data from (**A**) non-DN (*blue dots*) and micro-DN (*pink triangles*) samples and (**B**) non-DN (*blue dots*) and macro-DN (*red triangles*) samples. The *ellipse* in each figure indicates the Hotelling T2 (0.95) range for this model

Table 2 The 19 serum biomarker candidates that statistically differentiated the different DN stages

MID	Mode[a]	*m/z*	Non-DN	Micro-DN	Macro-DN	*p* value	Formula	Metabolite
11	C	114.067	0.501±0.153	0.612±0.209	1.052±0.506	<0.0001	$C_4H_7N_3O$	Creatinine
17	C	129.067	0.046±0.035	0.065±0.049	0.125±0.079	<0.0001	$C_5H_8N_2O_2$	
29	C	134.046	0.126±0.025	0.141±0.041	0.170±0.036	<0.0001	$C_4H_7NO_4$	Aspartic acid
39	C	146.118	0028±0.007	0.032±0.008	0.039±0.010	<0.0001	$C_7H_{16}NO_2$	γ-Butyrobetaine
51	C	156.139	0.006±0.005	0.005±0.004	0.001±0.003	0.0005	$C_9H_{17}NO$	
52	C	158.154	0.063±0.020	0.055±0.022	0.040±0.012	0.0007	$C_9H_{19}NO$	
69	C	176.104	0.194±0.053	0.199±0.060	0.275±0.081	0.0005	$C_6H_{13}N_3O_3$	Citrulline
78	C	203.150	0.006±0.002	0.007±0.002	0.010±0.005	0.0004	$C_8H_{18}N_4O_2$	SDMA
82	C	209.093	0.010±0.004	0.011±0.005	0.016±0.005	0.0002	$C_{10}H_{12}N_2O_3$	Kynurenine
96	C	243.184	0.026±0.013	0.019±0.012	0.015±0.007	0.0301		
97	C	244.106	0.0006±0.001	0.0009±0.001	0.002±0.002	0.0003		
114	C	276.128	0.008±0.006	0.006±0.004	0.003±0.003	0.0104		
127	C	302.197	0.106±0.050	0.079±0.047	0.062±0.028	0.0372		
134	C	316.213	0.010±0.009	0.006±0.007	0.003±0.002	0.0158		
152	A	96.960	0.216±0.063	0.243±0.063	0.341±0.103	<0.0001		
158	A	103.014	0.003±0.002	0.004±0.002	0.005±0.002	0.0001	$C_2H_4N_2O_3$	
202	A	149.049	0.030±0.006	0.034±0.009	0.051±0.019	<0.0001	$C_6H_6N_4O$	
232	A	187.098	0.020±0.013	0.017±0.011	0.009±0.004	<0.0001	$C_9H_{16}O_4$	Azelaic acid
246	A	209.031	0.029±0.012	0.024±0.009	0.016±0.013	<0.0001	$C_6H_{10}O_8$	Galactaric acid

[a] Mode "C" and "A" indicate that the candidate metabolites were obtained in cationic and anionic analysis, respectively

The relative ratio of peak area of each metabolite is shown as the mean±SD

$0.792\pm1.21\times10^{-2}$) in the cross-validation test. In a bootstrap test, the AUCs were 0.875±0.0419 and 0.820±0.0543 for training and cross-validation, respectively. These results indicate that the developed model is sufficiently accurate, specific, and general.

Table 3 AUC values for individual markers

Metabolite	AUC	95 % CI		*p* value
Creatinine	0.7526	0.6423	0.8629	8.06×10^{-4}
MID 17	0.7319	0.6128	0.851	2.09×10^{-3}
Aspartic acid	0.7069	0.5871	0.8267	6.05×10^{-3}
γ–Butyrobetaine	0.7379	0.6149	0.8609	1.60×10^{-3}
MID 51	0.644	0.5021	0.7858	0.0561
MID 52	0.7078	0.5853	0.8302	5.84×10^{-3}
Citrulline	0.6431	0.5158	0.7704	0.0576
SDMA	0.731	0.6098	0.8522	2.18×10^{-3}
Kynurenine	0.7284	0.6122	0.8447	2.44×10^{-3}
MID 96	0.6828	0.5475	0.818	0.0153
MID 97	0.6655	0.5396	0.7914	0.0281
MID 114	0.6836	0.5399	0.8274	0.0148
MID 127	0.6707	0.5321	0.8093	0.0235
MID 134	0.6552	0.5102	0.8001	0.0395
MID 152	0.7302	0.6048	0.8555	2.26×10^{-3}
MID 158	0.7108	0.5809	0.8407	5.16×10^{-3}
MID 202	0.7647	0.6492	0.8801	4.47×10^{-4}
Azelaic acid	0.731	0.6151	0.8469	2.18×10^{-3}
Galactaric acid	0.7591	0.6169	0.9012	5.89×10^{-4}

Discussion

The aim of this study was to obtain metabolic markers for early detection of DN from patient serum samples. We used CE-MS-based metabolome analysis to find differences in the serum metabolites from non-DN, micro-DN, and macro-DN samples. OPLS-DA with 289 metabolites clearly separated non-DN from macro-DN. Adequate separation of micro-DN from non-DN was also achieved. These results show that OPLS-DA is useful in this type of analysis. The resultant S-plot of the developed OPLS-DA model identified 19 metabolites that were major contributors to the separation of macro-DN from non-DN ($|p(corr)|>0.5$). These metabolites showed a gradual increase or decrease with progressive development of nephropathy. Among them, eight metabolites were identified, and these markers are discussed in comparison with other published reports below.

The concentration of serum creatinine was significantly increased in the micro-DN and macro-DN groups compared with the non-DN group ($p<0.0001$), and positively correlated with UACR ($r=0.5701$, $p<0.0001$) and negatively correlated

Table 4 Correlation analysis between the 19 biomarker candidates and clinical parameters (urinary albumin-to-creatinine ratio (UACR) or estimated glomerular filtration rate (eGFR))

MID	Metabolite	UACR		eGFR	
		Coefficients	*p* value	Coefficients	*p* value
11	Creatinine	0.5701	<0.0001[a]	−0.8832	<0.0001[a]
17		0.4968	<0.0001[a]	−0.5808	<0.0001[a]
29	Aspartic acid	0.4993	<0.0001[a]	−0.3912	0.0004[a]
39	γ-Butyrobetaine	0.4942	<0.0001[a]	−0.6492	<0.0001[a]
51		0.4728	<0.0001[a]	0.2204	<0.0001[a]
52		−0.4871	<0.0001[a]	−0.0678	0.053
69	Citrulline	0.4300	<0.0001[a]	−0.6531	<0.0001[a]
78	SDMA	0.4820	<0.0001[a]	−0.7111	<0.0001[a]
82	Kynurenine	0.5351	<0.0001[a]	−0.5627	<0.0001[a]
96		−0.3085	0.006[b]	0.1975	0.083
97		0.5223	<0.0001[a]	−0.7651	<0.0001[a]
114		−0.3638	0.001[b]	0.1392	0.224
127		−0.2961	0.009[b]	0.2035	0.074
134		−0.3669	0.001[a]	0.2397	0.035[c]
152		0.5336	<0.0001[a]	−0.7687	<0.0001[a]
158		0.4980	<0.0001[a]	−0.6302	<0.0001[a]
202		0.6352	<0.0001[a]	−0.7455	<0.0001[a]
232	Azelaic acid	−0.5210	<0.0001[a]	0.3739	0.0007[a]
246	Galactaric acid	−0.4596	<0.0001[a]	0.4152	0.0002[a]

[a] $p<0.001$
[b] $p<0.01$
[c] $p<0.05$

with eGFR (r=–0.8832, $p<0.0001$). Accumulation of serum creatinine was also observed in DN patients by metabolic analysis [19]. In clinical practice, creatinine is widely used as a marker of DN that reflects the renal function. Although serum creatinine had high specificity for detecting decreased GFR, the sensitivity is not sufficient because its levels do not significantly increase until the GFR is reduced to less than 50 % of normal levels [20].

The levels of amino acids, including aspartic acid ($p<0.0001$), citrulline (p=0.0005), SDMA (p=0.0004), and kynurenine (p=0.0002), were significantly elevated in the DN groups compared with the non-DN group. These metabolites showed high positive correlations with UACR (aspartic acid, r=0.4993, $p<0.0001$; citrulline, r=0.4300, $p<0.0001$; SDMA, r=0.4820, $p<0.0001$; kynurenine, r=0.5351, $p<0.0001$) and negative correlations with eGFR (aspartic acid, r=–0.3912, p=0.0004; citrulline, r=–0.6531, $p<0.0001$; SDMA, r=–0.7111, $p<0.0001$; kynurenine, r=–0.5627, $p<0.0001$). Aspartic acid and citrulline are involved in the urea cycle. Urea, is a major end product of

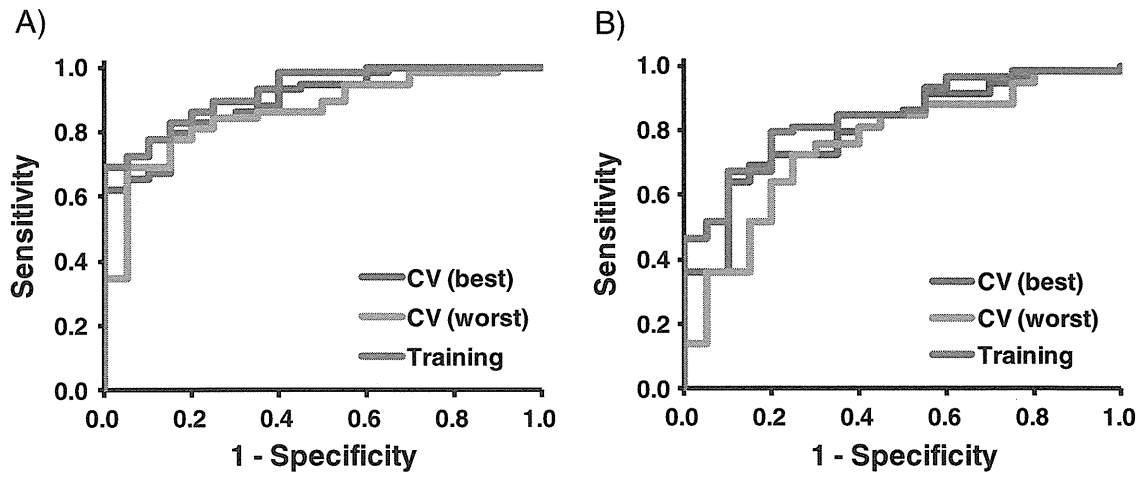

Fig. 2 ROC curve analyses in combination with (**A**) γ-butyrobetaine, SDMA, azelaic acid, MID 114, and MID 127, and (**B**) aspartic acid, SDMA, azelaic acid, and galactaric acid to discriminate non-DN and DN patients

nitrogen metabolism, and is produced by free ammonia and aspartic acid. Citrulline is normally taken up by the kidneys and converted to urea via arginine. Chuang et al. found significant accumulation of urea cycle intermediates in the patients with end-stage renal disease [21]. Because the kidneys are important in conversion of citrulline to arginine, the increase in the serum level of citrulline in DN patients could be attributed to degradation of this function.

SDMA and asymmetric dimethylarginine (ADMA), which is a structural isomer of SDMA, are formed by the enzymatic methylation of arginine residues within proteins. These metabolites have been identified as biomarkers for chronic kidney disease [22]. ADMA is metabolized by dimethylarginine dimethylaminohydrolase (EC 3.5.3.18) into citrulline and dimethylamine in the kidneys, whereas SDMA is excreted directly into the urine without further modification [23]. In this study, ADMA was under the detection limit, but SDMA was positively correlated with a decrease in function of kidney. Therefore, SDMA is a more sensitive marker than ADMA of various renal diseases, including DN.

Tryptophan is metabolized to kynurenine and further metabolized to acetyl-CoA and NAD in the tryptophan-kynurenine pathway. The rate limiting enzymes of this pathway are indoleamine 2,3-dioxygenase (EC 1.13.11.52) in the kidney and tryptophan 2,3-dioxygenase (EC 1.13.11.11) in the liver. Both these enzymes metabolize tryptophan to *N*-formylkynurenine, and *N*-formylkynurenine is subsequently catabolized to kynurenine. Saito et al. showed the peripheral kynurenine pathway accelerates in renal insufficient rats, and the reaction rate was positively correlated with the severity of the case [24]. They also found increased serum kynurenine concentrations reflected increased tryptophan 2,3-dioxygenase and decreased kynureninase (EC 3.7.1.3) activity in the liver [24]. Integration of profiling of these enzyme activities and metabolites will increase understanding of these mechanisms.

We detected a significant increase in γ-butyrobetaine in DN patients ($p<0.0001$). Toyohara et al. showed a negative correlation between γ-butyrobetaine and eGFR in plasma from the patients with chronic kidney disease [25]. Because γ-butyrobetaine is converted to L-carnitine by γ-butyrobetaine dioxygenase (EC 1.14.11.1), it is assumed the increased γ-butyrobetaine arises from inhibition of this enzyme in the kidney.

The levels of azelaic acid ($p<0.0001$) and galactaric acid ($p<0.0001$) were significantly lower in the DN groups than the non-DN group. These metabolites also showed high negative correlations with UACR (azelaic acid, $r=-0.5210$, $p<0.0001$; galactaric acid, $r=-0.4596$, $p<0.0001$) and positive correlations with eGFR (azelaic acid, $r=0.3739$, $p=0.0007$; galactaric acid, $r=0.4152$, $p=0.0002$). Azelaic acid is a saturated C9 dicarboxylic acid derived from oxidation of fatty acids and inhibits the generation of reactive oxygen species on neutrophils [26]. Galactaric acid, is a natural product found in various fruits, and acts as a growth substrate for many organisms, including *Escherichia coli* [27]. However, biological mechanisms of decreased serum azelaic acid and galactaric acid after onset DN need to be clarified.

In this study, the obtained 19 metabolites showed relatively high separation abilities (AUC values of receiver operating characteristic curves 0.643–0.765, Table 3). To increase the separation ability, we then applied a MLR model to this dataset. The developed MLR model included five metabolites, γ-butyrobetaine, SDMA, azelaic acid, MID 114, and MID 127. This model had a higher AUC value for diagnosis of DN (0.927, $p<0.0001$) than single markers, and shows the use of multiple markers is advantageous (Fig. 2a). However, this model contained two unidentified metabolites. The model using only identified metabolites was even simpler and more versatile for actual diagnosis because it could be used with quantification by another technique, such as LC, LC-MS, or an enzymatic method. Thus, we developed another MLR model using only the identified metabolites, aspartic acid, SDMA, azelaic acid and galactaric acid (Fig. 2b). This model showed high separation ability (AUC value 0.844, $p<0.0001$), and could also be used to diagnose DN. However, there are several limitations to be acknowledged for this study. For example, the developed model should be further validated using larger and independent new datasets. In addition, although we evaluated the generalization ability of the developed model using cross-validation, the specificity of the model was not assessed. Especially, the specificity for DN using data obtained from study of other kidney diseases (e.g., kidney cancer) should be addressed in future study.

In conclusion, we applied CE-MS-based metabolome profiling to serum samples from diabetic patients with or without existing DN. Biomarker candidates for the early diagnosis of DN were obtained. Although a further validation study is needed, this technique has potential as a tool for biomarker discovery studies.

Acknowledgments We thank Dr. Astuko Watarai, Japan Labour Health and Welfare Organization Chubu Rosai Hospital, for assistance with sample collection. We also thank Maki Sugawara and Hiroko Ueda, Institute for Advanced Biosciences, Keio University, and Jiro Nakamura, Department of Endocrinology and Diabetes, Nagoya University Graduate School of Medicine, for technical support and fruitful discussions. This work was supported by a Health and Labour Sciences Research Grant "Research on Biological Markers for New Drug Development", Grants from the Ministry of Health, Labour and Welfare of Japan "Research on Rare and Intractable Disease", KAKENHI Grants-in-Aid for Scientific Research on Priority Areas "Systems Genomes" and "Lifesurveyor" from the Ministry of Education, Culture, Sports, Science and Technology of Japan, and research funds from the Yamagata prefectural government and the City of Tsuruoka.

References

1. Gross JL, de Azevedo MJ, Silveiro SP, Canani LH, Caramori ML, Zelmanovitz T (2005) Diabetic nephropathy: diagnosis, prevention, and treatment. Diabetes Care 28(1):164–176
2. Kim HJ, Cho EH, Yoo JH, Kim PK, Shin JS, Kim MR, Kim CW (2007) Proteome analysis of serum from type 2 diabetics with nephropathy. J Proteome Res 6(2):735–743
3. Molitch ME, DeFronzo RA, Franz MJ, Keane WF, Mogensen CE, Parving HH, Steffes MW (2004) Nephropathy in diabetes. Diabetes Care 27(Suppl 1):S79–S83
4. Tabaei BP, Al-Kassab AS, Ilag LL, Zawacki CM, Herman WH (2001) Does microalbuminuria predict diabetic nephropathy? Diabetes Care 24(9):1560–1566
5. Dihazi H, Muller GA, Lindner S, Meyer M, Asif AR, Oellerich M, Strutz F (2007) Characterization of diabetic nephropathy by urinary proteomic analysis: identification of a processed ubiquitin form as a differentially excreted protein in diabetic nephropathy patients. Clin Chem 53(9):1636–1645
6. Mischak H, Kaiser T, Walden M, Hillmann M, Wittke S, Herrmann A, Knueppel S, Haller H, Fliser D (2004) Proteomic analysis for the assessment of diabetic renal damage in humans. Clin Sci (Lond) 107(5):485–495
7. Tiziani S, Lopes V, Gunther UL (2009) Early stage diagnosis of oral cancer using 1H NMR-based metabolomics. Neoplasia 11(3):269–276
8. Kind T, Tolstikov V, Fiehn O, Weiss RH (2007) A comprehensive urinary metabolomic approach for identifying kidney cancer. Anal Biochem 363(2):185–195
9. Sieber M, Wagner S, Rached E, Amberg A, Mally A, Dekant W (2009) Metabonomic study of ochratoxin a toxicity in rats after repeated administration: phenotypic anchoring enhances the ability for biomarker discovery. Chem Res Toxicol 22(7):1221–1231
10. Hirayama A, Kami K, Sugimoto M, Sugawara M, Toki N, Onozuka H, Kinoshita T, Saito N, Ochiai A, Tomita M, Esumi H, Soga T (2009) Quantitative metabolome profiling of colon and stomach cancer microenvironment by capillary electrophoresis time-of-flight mass spectrometry. Cancer Res 69(11):4918–4925
11. Soga T, Baran R, Suematsu M, Ueno Y, Ikeda S, Sakurakawa T, Kakazu Y, Ishikawa T, Robert M, Nishioka T, Tomita M (2006) Differential metabolomics reveals ophthalmic acid as an oxidative stress biomarker indicating hepatic glutathione consumption. J Biol Chem 281(24):16768–16776
12. Sugimoto M, Wong DT, Hirayama A, Soga T, Tomita M (2010) Capillary electrophoresis mass spectrometry-based saliva metabolomics identified oral, breast and pancreatic cancer-specific profiles. Metabolomics 6(1):78–95
13. Xia JF, Liang QL, Hu P, Wang YM, Li P, Luo GA (2009) Correlations of six related purine metabolites and diabetic nephropathy in Chinese type 2 diabetic patients. Clin Biochem 42(3):215–220
14. Jiang Z, Liang Q, Luo G, Hu P, Li P, Wang Y (2009) HPLC-electrospray tandem mass spectrometry for simultaneous quantitation of eight plasma aminothiols: application to studies of diabetic nephropathy. Talanta 77(4):1279–1284
15. Zhang J, Yan L, Chen W, Lin L, Song X, Yan X, Hang W, Huang B (2009) Metabonomics research of diabetic nephropathy and type 2 diabetes mellitus based on UPLC-oaTOF-MS system. Anal Chim Acta 650(1):16–22
16. Soga T, Ohashi Y, Ueno Y, Naraoka H, Tomita M, Nishioka T (2003) Quantitative metabolome analysis using capillary electrophoresis mass spectrometry. J Proteome Res 2(5):488–494
17. Soga T, Igarashi K, Ito C, Mizobuchi K, Zimmermann HP, Tomita M (2009) Metabolomic profiling of anionic metabolites by capillary electrophoresis mass spectrometry. Anal Chem 81(15):6165–6174
18. Witten I, Frank E (2000) Data mining: practical machine learning algorithms with Java implementations. Morgan Kaufmann Publishers, CA
19. Xia JF, Liang QL, Liang XP, Wang YM, Hu P, Li P, Luo GA (2009) Ultraviolet and tandem mass spectrometry for simultaneous quantification of 21 pivotal metabolites in plasma from patients with diabetic nephropathy. J Chromatogr B Analyt Technol Biomed Life Sci 877(20–21):1930–1936
20. Perrone RD, Madias NE, Levey AS (1992) Serum creatinine as an index of renal function: new insights into old concepts. Clin Chem 38(10):1933–1953
21. Chuang CK, Lin SP, Chen HH, Chen YC, Wang TJ, Shieh WH, Wu CJ (2006) Plasma free amino acids and their metabolites in Taiwanese patients on hemodialysis and continuous ambulatory peritoneal dialysis. Clin Chim Acta 364(1–2):209–216
22. Fleck C, Janz A, Schweitzer F, Karge E, Schwertfeger M, Stein G (2001) Serum concentrations of asymmetric (ADMA) and symmetric (SDMA) dimethylarginine in renal failure patients. Kidney Int 59:S14–S18
23. Pahlich S, Zakaryan RP, Gehring H (2006) Protein arginine methylation: cellular functions and methods of analysis. Biochim Biophys Acta 1764(12):1890–1903
24. Saito K, Fujigaki S, Heyes MP, Shibata K, Takemura M, Fujii H, Wada H, Noma A, Seishima M (2000) Mechanism of increases in L-kynurenine and quinolinic acid in renal insufficiency. American Journal of Physiology-Renal Physiology 279(3):F565
25. Toyohara T, Akiyama Y, Suzuki T, Takeuchi Y, Mishima E, Tanemoto M, Momose A, Toki N, Sato H, Nakayama M, Hozawa A, Tsuji I, Ito S, Soga T, Abe T (2010) Metabolomic profiling of uremic solutes in CKD patients. Hypertens Res 33 (9):944–952
26. Akamatsu H, Komura J, Asada Y, Miyachi Y, Niwa Y (1991) Inhibitory effect of azelaic acid on neutrophil functions: a possible cause for its efficacy in treating pathogenetically unrelated diseases. Arch Dermatol Res 283(3):162–166
27. Watanabe S, Yamada M, Ohtsu I, Makino K (2007) α-Ketoglutaric semialdehyde dehydrogenase isozymes involved in metabolic pathways of D-glucarate, D-galactarate, and hydroxy-L-proline. J Biol Chem 282(9):6685

Macrophage-mediated glucolipotoxicity via myeloid-related protein 8/toll-like receptor 4 signaling in diabetic nephropathy

Takashige Kuwabara, Kiyoshi Mori, Masashi Mukoyama, Masato Kasahara, Hideki Yokoi & Kazuwa Nakao

Clinical and Experimental Nephrology
Official Publication of the Japanese Society of Nephrology

ISSN 1342-1751

Clin Exp Nephrol
DOI 10.1007/s10157-013-0922-5

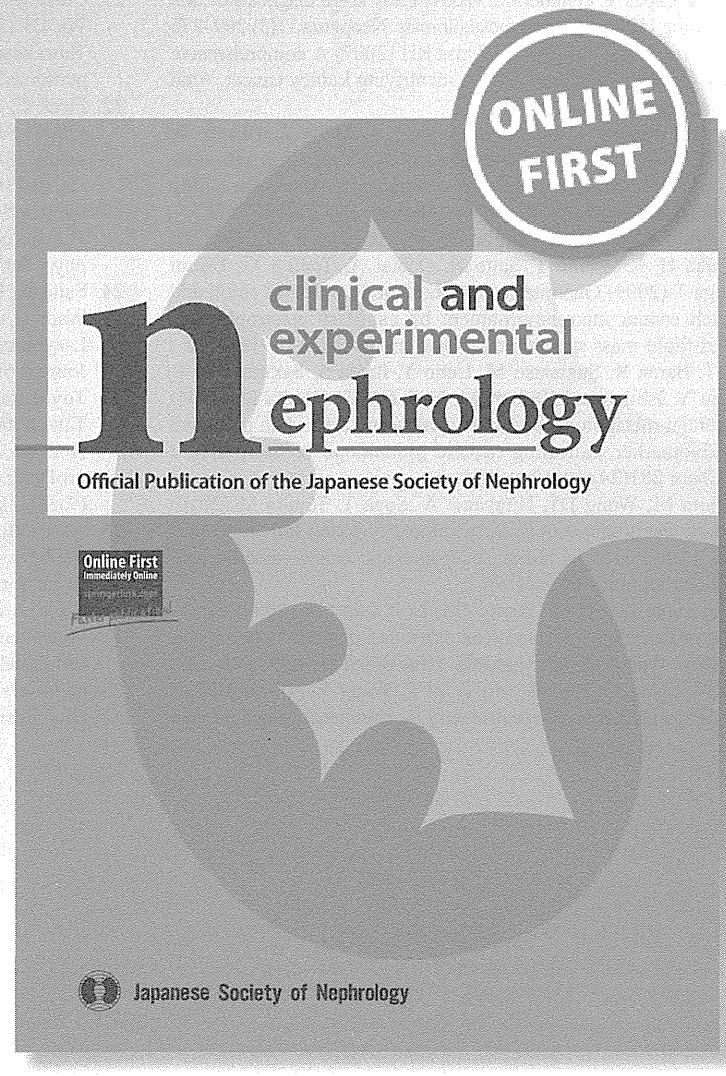

Springer